

Full Length Research Paper

Henna wood as an adsorptive material for bentazon

Brahmi Mounaouer^{2*}, Ahmed Wali¹, Olfa Fourti² and Abdennaceur Hassen²

¹Laboratory "Water, Energy and Environment" (LR3E), code: AD-10-02, Department of Materials, National Engineering School of Sfax, University of Sfax, B.P.W.3038, Sfax, Tunisia.

²Water Research and Technology Center, Borj Cédria Science and Technology Park, P.O. Box 273, Soliman 8020, Tunisia.

Received 4 July, 2013; Accepted 14 July, 2014

In this study, the efficiency of activated carbon produced from Henna wood was studied to remove herbicide from aqueous solutions by adsorption. The parameters that affect the adsorption such as contact time, activated carbon dosage, initial concentration of adsorbate, stirring rate, temperature, and pH on bentazon adsorption were studied. The use of Henna wood as a raw material to produce activated carbon by physical activation was investigated. The activated carbons produced were characterized by nitrogen adsorption isotherms and point of zero charge properties. Brunauer, Emmett and Teller (BET) surface area of the activated carbon was determined. The removal of herbicide from aqueous solutions by adsorption on activated carbon produced was studied. The results of the present investigation showed that activated carbons prepared from Henna wood have good adsorption capacity for the removal of bentazon from aqueous solution. The Langmuir model provides the best correlation of the experimental equilibrium data. Adsorption isotherm according to BET classification was of Type I. The adsorption isotherms of bentazon revealed that adsorption increased as the concentration increases up to a saturation point. Enthalpy, entropy and free enthalpy adsorption have a negative value indicating that the adsorption of bentazon on the Henna wood activated was feasible, spontaneous and exothermic at 20 to 40°C.

Key words: Activated carbon, adsorption, thermodynamic parameters, Henna wood, Bentazon.

INTRODUCTION

In areas where intensive monoculture is practiced, pesticide use has been the standard method for pest control. Unfortunately, the use of pesticides can also result in environmental

problems, such as disruption of predator-prey relationships and loss of biodiversity (Zhang et al., 2010). Additionally, the slow degradation of pesticides in the environment can

*Corresponding author. E-mail: brahmounaouer@yahoo.fr. Tel: +216 79412199. Fax: +216 79412802.

Abbreviations: **b**, Enthalpy of adsorption (L/mol); **BET**, Brunauer, Emmett and Teller; **C_i**, initial concentrations; **C_f**, final concentrations; **EPA**, environmental protection agency; **FTIR**, Fourier transfer infra-red; **HPLC**, high performance liquid chromatography; **GAC**, granular activated carbon; **ΔG**, free energy change; **ΔH**, enthalpy change; **k₁**, pseudo 1st order rate constant; **k₂**, pseudo 2nd order rate constant; **LWAC**, activated carbon prepared from *Lawsonia inermis* wood; **Q**, Langmuir adsorption capacity (mmol g⁻¹); **q_e**, the adsorption capacity (mol g⁻¹); **q_t**, the amount of adsorbate adsorbed at time t (mol g⁻¹); **rpm**, rounds per minute; **ΔS**, entropy change; **SEM**, scanning electron microscopy; **V**, volume of sample (mL); **μg**, micro gram; **μL**, micro-liter.

Author(s) agree that this article remain permanently open access under the terms of the [Creative Commons Attribution License 4.0 International License](https://creativecommons.org/licenses/by/4.0/)

lead to environmental contamination of water, soil, air, several kinds of crops, and Indirectly, of humans (Navalon et al., 2002). Pesticides are artificially synthesized, toxic pesticides in the environment can lead to environmental contamination of water, soil, air, several types of crops, bioaccumulative agents. The on-growing and uncontrolled use of pesticides to fight pests and improve agricultural production constitutes a risk for water quality (Zhu et al., 2006). Thus, pesticides have been detected by monitoring surface and underground waters. According to the European Union Directives and Regulations for drinking water hygiene, the maximum allowed concentration of total pesticides is $0.5 \mu\text{g dm}^{-3}$ (Zhang et al., 2010). Different types of pesticides can be found in water. The most frequently found pesticides are derivatives of urea, pyridazinone, phenoxy acetic acid, tryazin and the group of chlorinated pesticides (Arcury et al., 2001).

Pesticides can be eliminated from water in different ways, most frequently by adsorption on granular activated carbon (GAC) and/or by ozonization (Arcury et al., 2002). When GAC is saturated, it is usually regenerated and reused. In the majority of cases, spent GAC is thermally regenerated either on-site or transported to a thermal regeneration facility. During regeneration, the contaminants are transformed into less toxic byproducts and the sorption capacity of the carbon is re-established; thus, increasing the useful life of the GAC and the costs of water treatment are reduced (Cabrera and Leckie, 2009).

The adsorption process is being widely used by many researchers for the removal of inorganic and organic pollutants from contaminated streams. Commercially available activated carbon has been frequently employed for thousands of years in many adsorption processes for removal of impurities from liquids and gases (Chowdhury et al., 2011). It contains lot of graphite like microcrystalline unit linked together, similar to that of carbon black (Do, 1996). The effectiveness of activated carbon as an adsorbent is attributed to its unique properties including highly developed internal surface area between 500 and 2000 m^2/g , favorable pore size and high degree of surface reactivity due to presence of surface functional groups, especially oxygen groups (Ismadji and Bhatia, 2001). Their structure is complex and heterogeneous due to presence of micropores, mesopores and macro pores of different size and shape. Despite its extensive use in synthetic waste water treatment, commercial activated carbon remains an expensive material. Therefore, in recent years, the need for economical methods for elimination of pesticides from contaminated water has necessitated research interest towards the production of activated carbon from inexpensive agro based waste material (Choudhari et al., 2013). However, the adsorption property of activated carbon is highly influenced by its preparation conditions. The preparation variables of temperature, time and impregnation ratio will significantly change its surface area, pore size distribution and surface functional groups. Therefore, it is a challenge to

produce specific types of activated carbon which are suitable for certain applications.

Bentazon (3-isopropyl-1H-2,1,3-benzothiadiazin-4(3H)-one 2,2-dioxide), known by the trade name Basagran, is a selective post-emergence herbicide used to control many broadleaf weeds and sedges primarily by contact action in most gramineous and many large seeded leguminous crops such as alfalfa, beans, corn, peanuts, peas, asparagus, cereals, peppers, peppermint, rice and sorghum (Pourata et al., 2009). It is also used on two terrestrial non-food crops: ornamental lawns and turf. It has little effect on germinating seeds, and is not used pre-emergence (irrelevant) (Garrido et al., 1998).

In soil, Bentazon has an average soil half-life of 20 days and is often undetectable after 42 days. Soil microbes are responsible for rapid degradation of bentazon (Sims et al., 2009). In water, the soil organic carbon sorption coefficient, K_{oc} , is 34 mL/g, indicating a weak sorption to soil particles, and the solubility is 500 mg/L. Due to rapid microbial degradation and photodegradation, bentazon has a low leaching potential despite having a low K_{oc} and a high solubility. In surface water, bentazon photodegrades with a half-life of 63 h (Pappiernik et al., 2007).

Generally, the environmental fate of herbicides depends on the chemical transformations, degradation and transport. Transformation determines which herbicides are degraded in the environment, and how many pesticides and their metabolites (degradation products) are present in the environment, where and for how long (Fontecha et al., 2008). Indeed, it is necessary to remove them from wastewater. Activated carbon is the most widely used adsorbent because of its extended surface area, microporous structure, and high adsorption capacity related to its great degree of surface reactivity. Many reports have described the successful use of the activated carbon as an adsorbent for the purification of water (Pintar, 2005; Ania and Beguin, 2007).

Lawsonia inermis wood is a shrub or small tree frequently cultivated in dry tropical and subtropical zones, including North Africa, India, Sri Lanka and the Middle East (Chung et al., 2002). Several studies have been carried out using activated carbon as an adsorbent by two different activation methods, physical and chemical (Garrido et al., 1998). Physical activation implies the pyrolysis of the precursor followed by the activation with gases, such as carbon dioxide, air, steam or a mixture of them. Chemical activation consists of the pyrolysis at relatively low temperature under the presence of an activating agent.

The objective of this work was to study the removal of bentazon from aqueous solutions using activated carbon prepared from *L. inermis* wood (LWAC). The adsorbent was prepared and characterized by surface and pore structural characteristics, scanning electron microscopy (SEM) and Fourier transform infrared spectroscopy (FT-IR) analyses. The effects of contact time, initial concentration of bentazon, activated carbon dosage, stirring rate,

temperature and initial solution pH were studied. The removal capacity of LWAC was studied by fitting the adsorption data to kinetic and isotherm models. Desorption studies of the used LWAC were also undertaken.

In this study, activated carbon was produced by physical activation of Henna wood and characterized, regarding its textural and surface chemical properties. The thermodynamic parameters such as enthalpy, entropy and free enthalpy adsorption were also considered from the adsorption isotherms measurements.

MATERIALS AND METHODS

Adsorbent preparation

The stems of *L. inermis* were collected from the field in Gabes (Tunisia). Its geographical coordinates are 33° 53' 0" north and 10° 7' 0" east. These materials were firstly carbonized with distilled water to remove impurity such as sand and leaves and soluble and colored components, dried at 110°C for 12 h, crushed in a steel blender, and sieved to obtain a particle size in the range of 1-2 mm. Bentazon obtained from BASF Aktiengesellschaft, 67056 Ludwigshafen, Germany, was used as adsorbate. Distilled water was used in adsorption experiments.

Active carbon preparation

Activated carbons were prepared from Henna wood by carbonization under nitrogen flow and activation under water vapor. Carbonization was carried out in a vertical stainless-steel reactor (length 170 mm, interior diameter 22 mm) which was inserted into a cylindrical electric furnace Nabertherm (LT 5/11HA, Model 976 Gemini R, Lilienthal, Germany). The dried wood was placed into the reactor and heated from room temperature to 400°C at a constant heating rate of 10°C/min under nitrogen flow, then held at 400°C for 1 h. The samples were left to cool down after the carbonization. Activation was carried out in the same furnace. The charcoal obtained was then physically activated at 850°C for 2 h under a nitrogen flow (100 cm³/min) saturated in steam after passing through the water saturator heated at 80°C. The tenor steam was fixed at 0.395 kg H₂O /kg N₂. After activation, the sample was cooled to ambient temperature under N₂ flow rate. The produced activated carbon was then dried at 105°C overnight, ground and sifted to obtain a powder with a particle size smaller than 45 µm, and finally kept in hermetic bottle for subsequent uses.

Active carbon characterization

The surface area of the Henna wood was calculated from the BET equation (Brunauer–Emmett–Teller) within the 0.01-0.15 relative pressure range. Nitrogen adsorption/desorption isotherms were measured at 77 K on an automatic adsorption instrument (Quantachrome Instruments, Model Nova1000e series, USA) in relative pressure ranging from 10⁻⁶ to 0.999. Prior to the measurement, all the samples were crushed and powdered to shorten the time required for reaching equilibrium in the isotherm study and degassed at 250°C under nitrogen flow for 16 h.

The nitrogen adsorption-desorption isotherms were used to determine the following parameters: specific surface area SBET (according to the BET equation), total pore volume V_{tot} (calculated from the nitrogen uptake at relative pressure of 0.99 by assuming that the pores are then filled with liquid adsorbate (N₂)), total micropore volume V_{micro} , according to simplified equations (Nickolov and

Mehandjiev, 2000), total mesopore volume V_{mes} (determined by subtracting the micropore volume from the total pore volume) and external surface area were calculated by using the t-plot method of Lippens and de Boer (Lippens and de Boer, 1965). The surface morphology of the samples was examined using a scanning electron microscope (Philips XL30 microscope model, Chungmoon City, Cheju Island).

Fourier transform infrared spectroscopy (FTIR)

The surface functional groups of the prepared activated carbon were detected by Fourier Transform Infrared spectroscopy using Shimadzu FTIR 8400S. A spectrum was recorded in the mid-IR range from 4000 to 400 cm⁻¹ with a resolution of 1 cm⁻¹.

Point zero charge measurements (pHpzc)

Batch equilibrium technique was applied to determine the pH at the zero point of charge. By using the pH drift method (Faria et al., 2004), the pH at the potential zero charge (pHpzc) of various activated carbons was measured. The pH of a solution of 0.1 M NaCl was adjusted between 2-12 by using 0.01 mol L⁻¹ NaOH. Activated carbon sample (0.2000 and 0.6000 g) was added into 100 mL of NaCl solution in 250 mL flask. The flasks were sealed, to eliminate any contact with air and then left at ambient temperature. The final pH was recorded after the pH had stabilized (typically after 24 h). The point at which initial pH and final pH were the same value was determined by using the graph of final pH versus initial pH. This was taken as the pHpzc of the activated carbon.

Adsorption studies

Batch equilibrium studies

Adsorption tests were conducted in batch mode using different concentrations of bentazon varying from 8 to 84 mg/L. However, 100 ml of bentazon solutions were put in Erlenmeyer flasks (250 mL) and equal mass of 50 mg of the prepared activated carbon was added to each flask and kept in an isothermal shaker of 200 rpm at 20, 25, 30, and 35°C, respectively for 2 h to reach equilibrium (Omri et al., 2012). The pH of the maximum adsorption of these herbicides in solutions by the activated carbon prepared was estimated at 3.3 values. Aqueous samples were taken from the herbicide solution and the concentrations were evaluated. All samples were filtered prior to the analysis to minimize the interference caused by fine carbon particles.

The concentrations of pesticides in supernatant before and after adsorption were determined by spectrophotometry at a wavelength of 224 nm, using a Shimadzu UV-VIS spectrophotometer 1650. A previously established linear Beer-Lambert relationship was used in the concentration analysis. The equilibrium adsorption capacity Q_e (mg/g) at different concentrations was calculated according to Equation 1:

$$Q_e = \frac{(C_i - C_e) V}{m} \quad (1)$$

Where, C_i and C_e (mg/L) are the liquid-phase concentrations of bentazon at initial and equilibrium, respectively. V is the volume of the solution (L) and m is the mass of dry adsorbent used (g).

Adsorption isotherms

Successful application of the adsorption technique demands studies based on various adsorption isotherm models (Colak et al., 2009)

because adsorption isotherm models clearly depict the relationship of amount adsorbed by a unit weight of adsorbent with the concentration of adsorbent remaining in the medium at equilibrium. Thus following Freundlich and Langmuir isothermal models were applied to the experimental data.

The Freundlich model is based on the assumption that adsorption occurs on a heterogeneous adsorption surface having unequally available sites with different energies of adsorption (Colak et al., 2009) and is given by the relation:

$$Q_e = K_F C_e^{1/n} \quad (2)$$

Where, K_F is roughly indicator of the adsorption capacity and $1/n$ is the adsorption intensity. In general, as the K_F value increases the adsorption capacity of the adsorbent increases. The magnitude of the exponent $1/n$ marks a favorable adsorption and values of $n > 1$ indicate a favorable condition of adsorption (Malik, 2003). Equation 2 can be rearranged to linear form to give Equation 3:

$$\ln Q_e = \ln K_F + \frac{1}{n} \ln C_e \quad (3)$$

Where Q_e is the amount adsorbed (mol/g), and C_e is the equilibrium concentration of the adsorbate (mol/L). K_F and n , the Freundlich constants, are related to adsorption capacity and adsorption intensity, respectively. The slope ($1/n$) and intercept (K) of a log-log plot of Q_e versus C_e are determined.

The Langmuir isotherm assumes that the surface of any adsorbent material contains a fixed number of active sites and saturation of these active sites stops the adsorption of the adsorbate (Langmuir, 1918). This indicates that the adsorption occurs until a monolayer of adsorption is completed and after completion of adsorption, no more interaction between the adsorbent and adsorbate molecules takes place (Li et al., 2009). It was adapted to model isotherms and to calculate the bentazon adsorption capacities of the produced carbons. The Langmuir isotherm used for adsorption of bentazon from the aqueous solution is given by the following Equation 4:

$$Q_e = \frac{Q_m K_L C_e}{1 + K_L C_e} \quad (4)$$

Where, Q_e is the maximum amount of adsorption and corresponds to the complete monolayer coverage on the surface (mg/g), C_e is the adsorbate equilibrium concentration (mg/g) and K_L is the Langmuir constant (L/mg). Q_m represents a practical limiting adsorption capacity when the surface is fully covered with adsorbate molecules and aids in the comparison of adsorption performance. Equation (4) can be rearranged to linear form to give Equation 5:

$$\frac{C_e}{Q_e} = \frac{C_e}{Q_m} + \frac{1}{K_L Q_m} \quad (5)$$

Where, constants K_L and Q_m relates to the energy of adsorption and adsorption capacity and their values are obtained from the slope and intercept of the plot of C_e/Q_e versus C_e for different temperature. The linear nature of the plot shows that the adsorption follows the Langmuir isotherm. The value of K_L , which is a measure of heat of adsorption is utilized to calculate dimensionless separation parameter R_L (Weber and Chakraborti, 1974). Indeed, Weber and Chakraborti (1974) expressed the essential characteristics and the feasibility of the Langmuir isotherm in terms of a dimensionless

constant separation factor R_L , which is defined as:

$$R_L = \frac{1}{1 + K_L C_0} \quad (6)$$

Where, K_L is the Langmuir constant and C_0 is the initial concentration of herbicide. According to McKay et al. (1982), R_L values between 0 and 1 indicate favorable adsorption.

Calculation of thermodynamic parameters

The thermodynamic equilibrium constant (b) is obtained by calculating the apparent equilibrium constant (b') at different initial concentrations of bentazon and extrapolating to zero (Bhattacharya et al., 2006):

$$b' = \frac{C_a}{C_e} \quad (7)$$

Where, C_a is the concentration of bentazon on the adsorbent at equilibrium in mg/L and C_e is the equilibrium concentration of bentazon in solution in mg/L.

According to the biosorbent dependency on the structure and surface functional groups, temperature has an impact on the adsorption capacity to a certain extent. It is well known that a temperature change alters the adsorption equilibrium in a specific way determined by the exothermic or endothermic nature of a process. The Gibbs free energy change (ΔG_{ad}^0), enthalpy (ΔH_{ad}^0) and entropy change (ΔS_{ad}^0) are very important thermodynamic parameters of adsorption that can confirm the feasibility, spontaneity and heat change for the biosorption process. Parameters like Gibb's free energy (ΔG_{ad}^0), change in entropy (ΔS_{ad}^0), change in enthalpy (ΔH_{ad}^0), etc. have been calculated from the relations (Amin, 2009):

$$\Delta G_{ad}^0 = -RT \ln b, \quad (8)$$

$$\Delta H_{ad}^0 = -R(T_2 T_1 / T_2 - T_1) \times \ln(b_2 / b_1), \quad (9)$$

$$\Delta S_{ad}^0 = \Delta H_{ad}^0 - \Delta G_{ad}^0 / T, \quad (10)$$

Where, R is a universal gas constant, b , b_1 and b_2 are the Langmuir constants at 20, 25, 30 and 35°C, respectively, obtained from slopes and intercepts of Langmuir isotherms.

Integral enthalpy and entropy have been used to explain the bentazon adsorption. Generally, the entropy evolution is similar to the enthalpy. Integral enthalpy is needed to control integral entropy associated with the adsorption process. The negative values of free enthalpy indicate that adsorption is spontaneous.

RESULTS AND DISCUSSION

Characteristics of *L. inermis* wood-based activated carbon

Specific surface area and pore structure of LWAC

Identifying the pore structure of adsorbent, which is commonly determined by the adsorption of inert gases, is

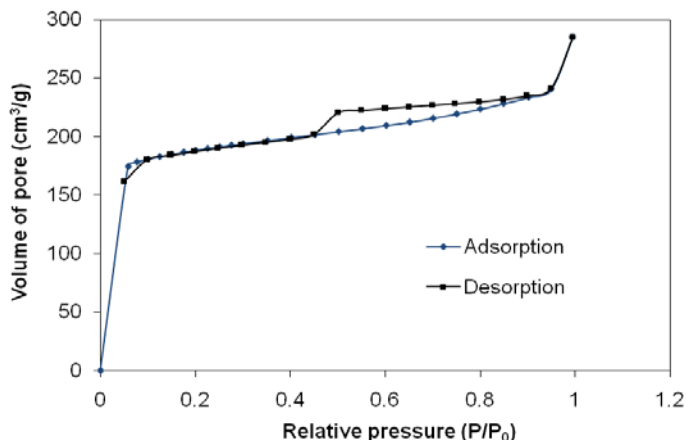


Figure 1. Adsorption-desorption isotherm of the activated carbon.

Table 1. Physical and chemical properties of the prepared activated carbon.

Parameter	Values
Specific surface area, S_{BET} (m^2/g)	584
Surface area micropore, S_{micro} (m^2/g)	483
External surface area, S_{ext} (m^2/g)	100
Micropore volume, V_{micro} (cm^3/g)	0.245
Total pore volume, V_T (cm^3/g)	0.441
Point zero charge (pH_{PZC})	11.32

an essential procedure before designing the adsorption process (Saritha et al., 2007). Figure 1 shows the adsorption-desorption isotherm of N_2 at 77 K. Adsorption data were obtained over the relative pressure, P/P_0 , range from 10^{-7} to 1. Table 1 presents the physical properties of Henna wood. The surface area of Henna wood was found to be $584 m^2/g$, which was much higher than conventional activated carbons, that is, activated carbons from olive-tree wood reconsidered ($474 m^2/g$) (Rajashekara et al., 2007), activated carbon from sawdust of Algarroba ($549 m^2/g$) (Ahmad et al., 2008) and wood coal-based activated carbon ($331 m^2/g$) (Maldonado et al., 2006).

The graph of the adsorption isotherm in Figure 2, is a Type I isotherm and this indicates that the activated carbon is microporous. Initial step region of the isotherm is abruptly followed by a plateau indicating that the adsorption has virtually stopped because multilayer of adsorbate cannot be formed due to close proximity of the pore wall. It can be seen from Table 1 that most pores of Henna wood are in the micropore range, the micropore volume (V_{micro}) occupies 55% of the total pore volume.

Surface morphology of LWAC

The SEM micrographs of LWAC sample are given in Figure 2 indicating that the porosity of the material was produced

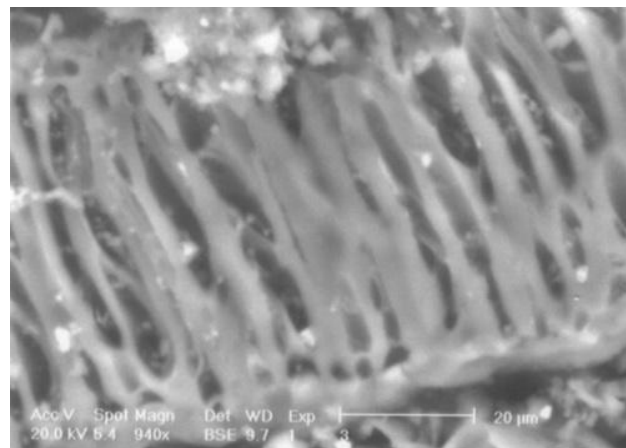


Figure 2. SEM image of Henna wood.

by attack of the reagent (H_2O) during activation. The increase in the steam tenor supports the following gasification process under high temperature (Ali and Gupta, 2006):



After undergoing carbonization and activation process, the volatile matter content decreased significantly whereas the fixed carbon content increased in Henna wood. This was due to the pyrolytic effect where most of the organic substances have been degraded and discharged as gas and liquid tars leaving a material with high carbon purity (Ren et al., 2011). Halim et al. (2010) found that increasing the carbonization temperature decreased the yield progressively due to release of volatile products as a result of intensifying dehydration and elimination reaction.

Function groups of LWAC

The FTIR spectrum of Henna wood is illustrated in Figure 3. A wide absorption band at $3200-3600 cm^{-1}$ with a maximum at about $3411 cm^{-1}$ is assigned to O-H stretching vibrations of hydrogen bonded hydroxyl groups (Wang et al., 2007). Aliphatic C-H stretching vibration is found as a very weak peak at $2884 cm^{-1}$ while asymmetric vibration of CH_2 group appears at $2915 cm^{-1}$. The bands located at about 1609 and $1414 cm^{-1}$ were attributed to carbonyl (e.g. ketone) and carboxylate ion (COO^-) groups, respectively. The shoulder at $1080 cm^{-1}$ can be ascribed to C-OH stretching of phenolic groups (Mourão et al., 2011).

Effect of adsorbent dosage and initial bentazon concentration

The adsorbent dosage is an important parameter because this parameter determines the capacity of

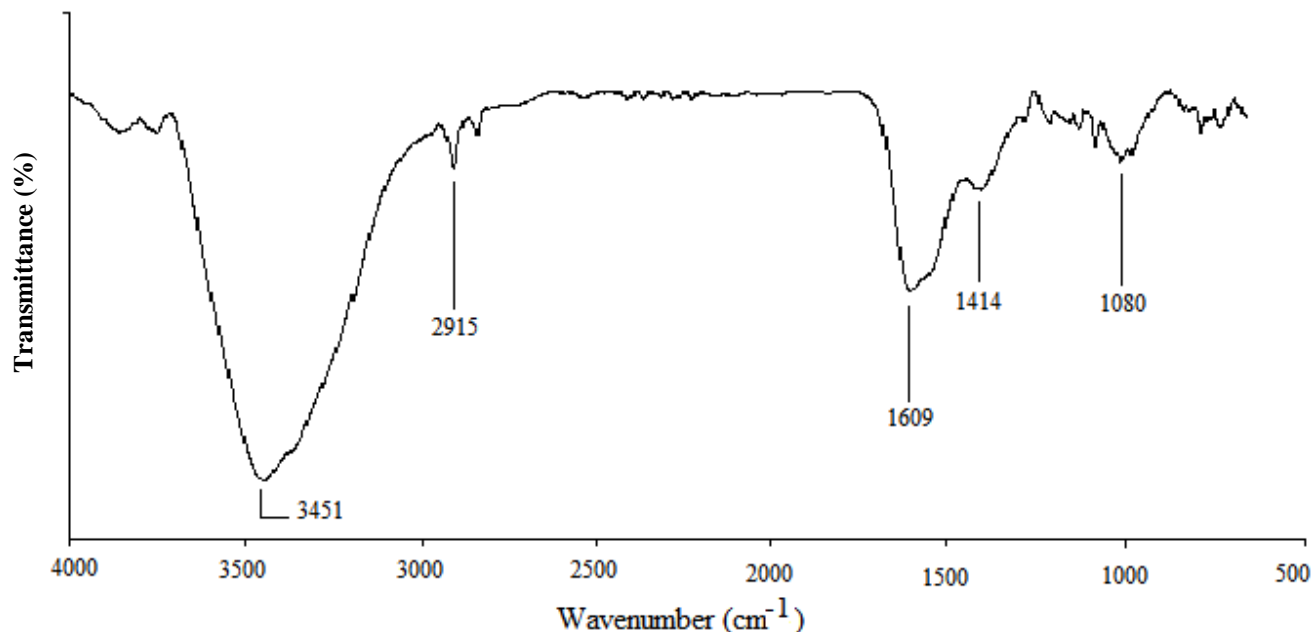


Figure 3. FTIR spectrum of the Henna wood.

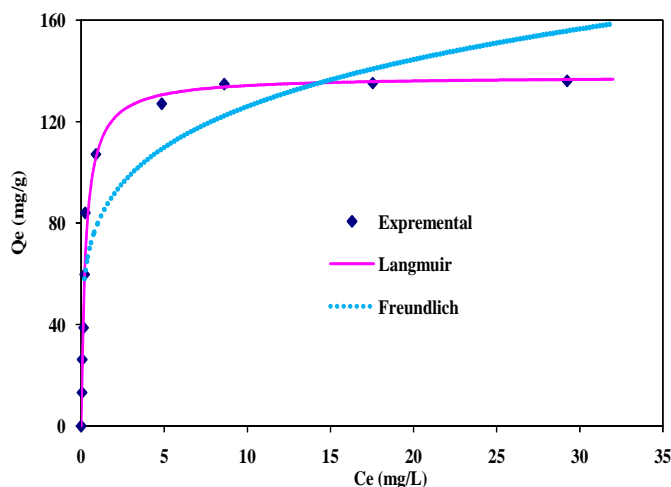


Figure 4. Adsorption isotherm of Basagron at 20°C fitted with Langmuir and Freundlich models. Q_e is the maximum amount of adsorption; C_e is the adsorbate equilibrium concentration (mg/L).

adsorbent for a given bentazon concentration and also determines sorbent-sorbate equilibrium of the system. From Figure 4, the removal of bentazon depends on the initial concentration of the adsorbate and the adsorbent dosage. For example, the percentage of removal of bentazon increased for the concentrations 22 and 78 mg/L, respectively, from 54 and 16.6% at 10 mg to 91 and 75% at 50 mg of adsorbent dose. The increased removal at high dosages is expected, because of the increased adsorbent surface area and availability of more adsorption

sites (Chung et al., 2002). The optimum dosage was found to be 50 mg.

The percentage removal of the bentazon was found to decrease with the increase in initial bentazon concentration at constant amount of adsorbent of about 50 mg. This indicates that there exist reductions in immediate solute adsorption, owing to the lack of available active sites required for the high initial concentration of bentazon. Similar results have been reported in literature (Al-Sehaibani, 2000; Dweck, 2002).

The percentage removal of the bentazon was found to decrease with the increase in initial bentazon concentration at constant amount of adsorbent of about 50 mg. This indicates that there exist reductions in immediate solute adsorption, owing to the lack of available active sites required for the high initial concentration of bentazon. Similar results have been reported in literature (Al-Sehaibani, 2000; Dweck, 2002).

Liquid phase adsorption

In the same focus, Ayranci and Hoda (2004) reported a Q_m value of 151 mg/g for adsorption of activated carbon-cloth. Bentazon isotherms were of type I according to the *International Union of Pure and applied Chemistry* (IUPAC) classification. This classification is in accordance with the characteristics of adsorbent.

However, activated carbon used in the present study has a high specific surface area (S_{BET} equal to 585 m²/g) and a microporous structure that explain the registered isotherms adsorption of Type I.

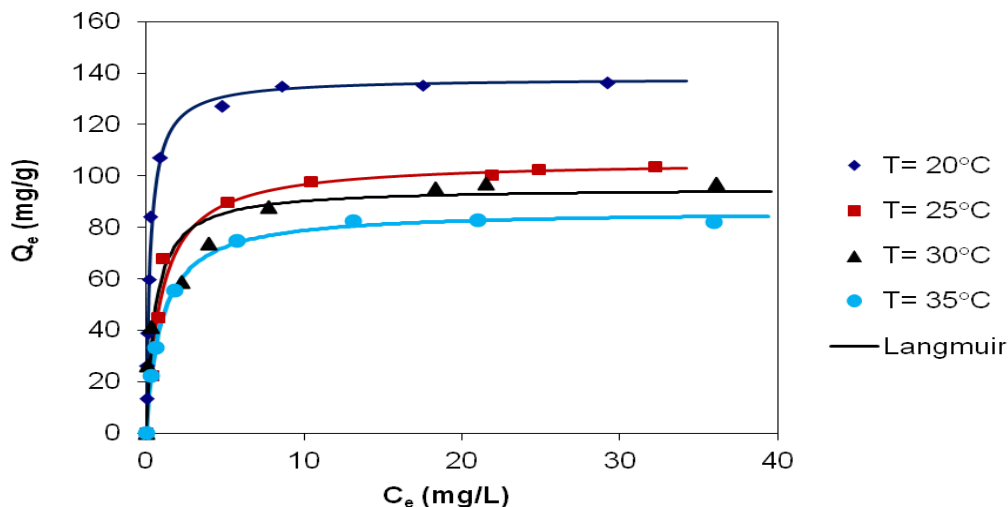


Figure 5. Adsorption isotherms of activated carbon at different temperatures fitted with Langmuir Model. Q_e is the maximum amount of adsorption; C_e is the adsorbate equilibrium concentration (mg/L).

Table 2. Langmuir constants for the adsorption of Basagran on the prepared activated carbon.

Temperature (°C)	Langmuir constants		
	Q_m (mg/g)	K_L (L/mg)	R^2
20	138.44	3.128	0.99
25	106.05	2.456	0.98
30	95.32	1.766	0.94
35	86.51	1.022	0.99

Q_m , Adsorption capacity (mg/g); K_L , Langmuir constant (L/mg); R^2 , correlation coefficient.

Thermodynamic features

Isotherms of adsorption

The removal of the herbicide with activated carbon was studied at different concentrations and according to variable temperatures of 20, 25, 30 and 35°C to determine the adsorption isotherms and the thermodynamic parameters. Figure 5 shows that the amount of adsorbed bentazon on activated carbon decreased as the temperature increased. For example, Q_m decreased from 136.7 to 84.4 mg/g by increasing temperatures of the solution from 20 to 35°C, respectively. This analysis appeared important to optimize the design of an adsorption.

However, Table 2 shows the results of calculated isotherm constants at different temperatures. The Langmuir isotherm models was found to be the best fit of the experimental data over all the concentration range as indicated by the high values of correlation coefficients ($R^2 = 0.99$).

The adsorption isotherms found was of a Type I according to BET classification (Brunauer et al., 1938). The Affinity of activated carbon to bentazon may be consented to the

high specific area of activated carbon, to the bentazon mobility in liquid phase as well as to the characteristic of activated carbon and the interaction forces (Vander Waals) between adsorbent and adsorbate. The isotherms results revealed the temperature dependence on the adsorptive behavior as shown in Figure 5. This result could be explained by the exothermic nature of the adsorption reaction. Langmuir constant showed its close dependence on the surrounding adsorption temperature, if the temperature increases the Langmuir constant decreases (Table 3).

Enthalpy and entropy of adsorption

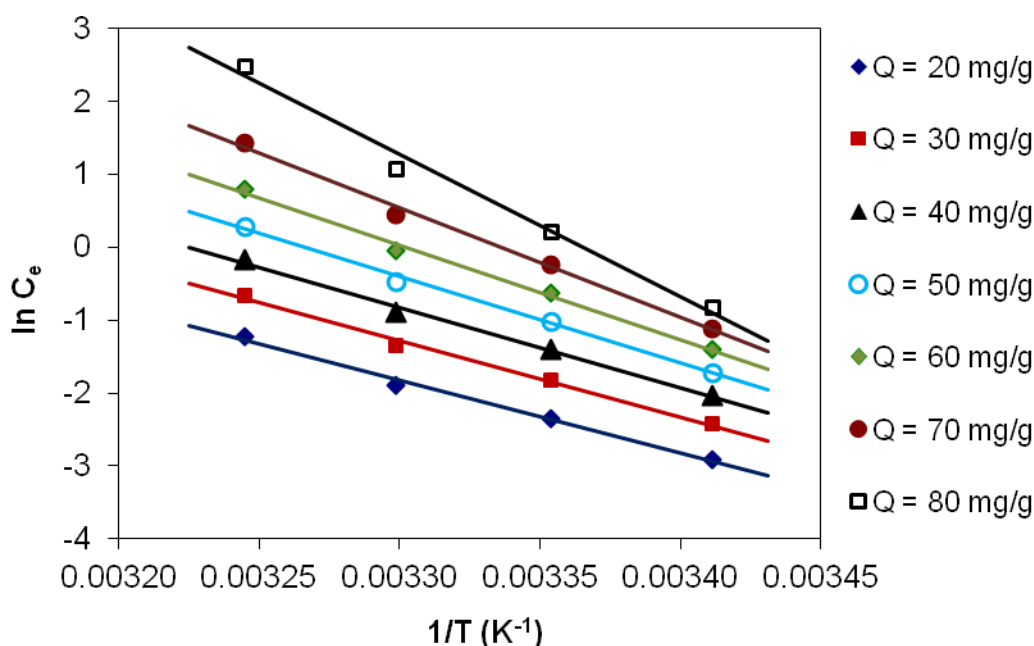
The variation of the equilibrium concentration according to the temperatures of enthalpy adsorption (ΔH_{ad}), or differential enthalpy is an indicator of the state of water adsorbed by the solid material (Tsami, 1991). The experimental data were calculated using Clausius-Claperyon equation (Kaymak-Ertekin and Gelik, 2004; Simal et al., 2007).

The experimental sorption isotherm in the form $\ln(C_e)$ versus $1/T$ is shown in Figure 6. The ΔH_{ad} was determined

Table 3. Thermodynamic features of the Basagran adsorption on the prepared activated carbon.

Q (mg/g)	$-\Delta H_{ad}$ (kJ/mol)	$-\Delta S$ (J/mol.K)	$-\Delta G$ (kJ/mol)
20	83.3	259.9	7.12
30	86.96	276.5	5.9
40	91.76	296.08	4.97
50	98.38	321.34	4.19
60	108.2	357.4	3.43
70	124.69	416.06	2.73
80	162.03	545.9	2.01

Q, Adsorbed quantity (mg/g); ΔH_{ad} , adsorption enthalpy (kJ/mol); ΔS_{ad} , adsorption entropy (J/mol.K); ΔG_{ad} , free enthalpy (kJ/mol).

**Figure 6.** Variation of the equilibrium concentration according to the temperatures. Q, Adsorbed quantity (mg/g); T, temperature; C_e , adsorbate equilibrium concentration (mg/L).

from the slop ($\Delta H_{ad}/R$). This procedure is based on the assumption that ΔH_{ad} is invariant with temperature (Tsami, 1991). The enthalpy of adsorption increased according to the adsorption capacity of the activated carbon (Table 3). Similar results for silica gel have been reported in literature (Malik, 2003). It has a negative value indicating that the process is exothermic in nature which is consistent with the results obtained earlier where the bentazon uptakes decrease with the increase in solution temperature. The values, variation of the equilibrium concentration according to the temperatures, of sorption are presented in Table 3. The values show a spontaneous and favorable adsorption.

The values of adsorption entropy are shown in Table 3. The negative value of entropy reflects decreasing random-

ness at the solid/solution interface with some structural changes in the adsorbate and adsorbent during the adsorption process.

The feasibility of the process is shown by negative values of free energy (Table 3). This parameters had a negative value ($-\Delta G$ (kJ/mol) and Q (mg/g) varying to 7.12 (kJ/mol) from 2.01(kJ/mol) and 20 (mg/g) to 80(mg/g) respectively), which explain why the phenomenon of adsorption of bentazon by activated carbon is spontaneous nature of the adsorption processes at the range of temperature study. The decrease in the value of the free energy with increase in the temperature suggests that adsorption is favored more at the lower temperature. The exothermic nature of the process is further confirmed by the negative value of enthalpy. The negative value of

Table 4. Separation Factor RL

RL value	Type of isotherm	RL (obtained)
RL > 1	Unfavorable	-
RL = 1	Linear	-
0 < RL < 1	Favorable	0.472
RL = 0	Irreversible	-

Table 5. Macro- and micro-pore diffusion rate constants.

Adsorbate concentration (mg/L)	Rate constants, Intraparticle rate parameter (mg/g·min ^{0.5})		
	K ₁	K ₂	K ₃
50	2.07	0.83	0.011

entropy change indicates decrease in the dye concentration at the solid-solution interface.

The negative ΔG values determine that the reaction rate is increasing with a decrease in temperature. However, an increase of the adsorbed quantity is accompanied by a decrease in the free enthalpy that could be explained by the adsorption tendency towards the thermodynamic equilibrium.

According to McKay et al. (1982) to express the essential characteristics and the feasibility of the Langmuir isotherm in terms of a dimensionless constant separation factor RL, the data obtained represent a favorable adsorption in the case of adsorption of bentazon (RL = 0.472). The shape of isotherm is given by the value of RL as given in Table 4.

Intraparticle and pore diffusion plots for adsorption of bentazon

Besides adsorption at the outer surface, there is also possibility of intraparticle diffusion from the outer surface into the pores of the material. The adsorption mechanism of a sorbate onto the adsorbent follows three steps viz. film diffusion, pore diffusion and intraparticle transport (Pant and Singh, 2004). Though there is a high possibility for pore diffusion to be the rate-limiting step in a batch process, the adsorption rate parameter which controls the batch process for most of the contact time is the intraparticle diffusion (Allen et al., 1989). Thus, to evaluate the rate controlling step a plot was drawn between amount of bentazon adsorbed on activated carbon (time)^{1/2} (graph not shown). The general shape of this curve that has not been advanced at this stage, showed three slopes. The first part of the curve is attributed to mass transfer effects (slope K₁) taking place with boundary layer diffusion, while the final linear parts indicate intraparticle diffusion (slope K₂ and K₃). The diffusion rate parameters K₁, K₂

and K₃ as obtained as shown in Table 5. The values for K₂ and K₃ indicate that the pores are micro-pores and the intraparticle diffusional resistance is due to micro-pores only (Singh et al., 2008). The diffusion rate parameters indicate that the intraparticle diffusion controls the sorption rate; which is the slowest step in adsorption.

Conclusions

The results of the present investigation showed that activated carbons prepared from Henna wood have good adsorption capacity for the removal of bentazon from aqueous solution. The adsorption characteristic has been examined with the variations in the parameters of pH, contact time, activated carbon dosage, stirring rate, initial bentazon concentration and temperature. The experimental data were analyzed using Langmuir and Freundlich isotherm models. The Langmuir model provides the best correlation of the experimental equilibrium data. Adsorption isotherm according to BET classification was of Type I.

The adsorption isotherms of bentazon are determined at different temperatures using Langmuir models. These isotherms revealed that adsorption increased as the concentration increases up to a saturation point.

Enthalpy, entropy and free enthalpy adsorption have a negative value indicating that process adsorption is exothermic, with the increase of the order degree and the spontaneous nature of the adsorption. Thermodynamic parameters suggested that the adsorption of bentazon on the Henna wood activated was feasible, spontaneous and exothermic in nature.

Conflict of Interests

The author(s) have not declared any conflict of interests.

REFERENCES

- Ahmad AL, Tan LS, Shukor SRA (2008). Dimethoate and atrazine retention from aqueous solution by nanofiltration membranes. *J. Hazard. Mater.* 151:71-77.
- Ali I, Gupta VK (2006). Advances in water treatment by adsorption technology. *Nat. Protoc.* 1: 2661-2667.
- Allen S, McKay G, Khader K (1989). Intraparticle diffusion of basic dye during adsorption onto Sphagnum Peat. *J. Environ. Pollut.* 50:9-50.
- Al-Sehaibani H (2000). Evaluation of extraction of Henna leaves as environmentally friendly corrosion inhibitor for metals. *Materialwiss. Werkstofftech.* 31:1060-1063.
- Amin NK (2009). Removal of direct blue-106 dye from aqueous solution using new activated carbons developed from pomegranate peel: adsorption equilibrium and kinetics. *J. Hazard. Mater.* 165:52-62.
- Ania CO, Beguin F (2007). Mechanism of adsorption and electrosorption of bentazon on activated carbon cloth in aqueous solutions. *Water. Res.* 41:3372-3380.
- Arcury TA, Quandt SA, Cravey AJ, Elmore RC, Russell GB (2001). "Farmworker reports of pesticide safety and sanitation in the work environment. *Am. J. Ind. Med.* 39:487-498.
- Arcury TA, Quandt SA, Russell GB (2002). "Pesticide safety among farmworkers: Perceived risk and perceived control as factors reflecting environmental justice. *Environ. Health. Perspect.* 110:233-

- 240.
- Ayranci E, Hoda N (2004). Adsorption of bentazon and propanil from aqueous solutions at the high area activated carbon-cloth. *Chem.* 57:755-762.
- Bhattacharya AK, Mandal SN, Das SK (2006). Adsorption of Zn (II) from aqueous solution by using different adsorbents. *Chem. Engr J.* 123:43-51.
- Brunauer S, Emmett PH, Teller E (1938). Adsorption of gases in multimolecular layers. *J. Am. Chem. Soc.* 60:309-319.
- Cabrera NL, Leckie JO (2009). Pesticide risk communication, risk perception, and self-protective behaviors among farmworkers in California's Salinas Valley. *Hispanic. J. Behav. Sci.* 31:258-272.
- Choudhari D, Sharma D, Phadnis A (2013). Heavy metal remediation of wastewaters with agrowastes. *Eur. Chem. Bull.* 2:880-886.
- Chowdhury ZZ, Zain SM, Khan RA, Ahmad AA, Islamand MS, Arami-Niya A (2011). Application of central composite design for preparation of Kenaf fiber based activated carbon for adsorption of manganese (II) ion. *Int. J. Phys. Sci.* 6:1-12.
- Chung WH, Chang YC, Yang LJ, Hung SI, WR, Wong JY, Lin et al (2002). Clinicopathologic features of skin reactions to temporary tattoos and analysis of possible causes. *Arch. Dermatol.* 138:88-92.
- Colak F, Atar N, Olgun A (2009). Biosorption of acidic dyes from aqueous solution by *Paenibacillus macerans*: Kinetic, thermodynamic and equilibrium studies. *Chem. Eng. J.* 150:122-130.
- Do DD (1996). A Model for Surface Diffusion of Ethane and Propane in Activated Carbon. *Chem. Eng. Sci.* 51:4145-4158.
- Dweck AC (2002). Natural ingredients for colouring and styling. *Int. J. Cosmet. Sci.* 24:287-302.
- Faria PCC, Orfao JJM, Pereira MFR (2004). Adsorption of anionic and cationic dyes on activated carbons with different chemistries. *Water. Res.* 38:2043-2052.
- Fontecha-Camara MA, Lopez-Ramo MV, Pastrana-Martinez LM (2008). Kinetics of diuron and amitrole adsorption from aqueous solution on activated carbons. *J. Hazard. Mater.* 156:472-477.
- Garrido EM, Lima JLC, Delerue-Matos CM, Brett AMO (1998). Electrochemical oxidation of bentazon at a glassy carbon electrode application to the determination of a commercial herbicide. *Talanta.* 46:1131-1135.
- Halim AA, Aziz HA, Johari MAM, Ariffin KS (2010). Comparison study of ammonia and COD adsorption on zeolite, activated carbon and composite materials in landfill leachate treatment. *Desalination.* 262:31-35.
- Ismadji S, Bhatia SK (2001). Characterization of activated carbons using liquid phase adsorption. *Carbon.* 39:1237-1250.
- Kaymak-Ertekin F, Gelik A (2004). Sorption isotherms and isosteric heat of sorption for grapes. *Lebensm. Wiss. Technik.* 37:429-438.
- Langmuir L (1918). The adsorption of gases on plane surface of glass, mica and platinum. *Am. Chem. Soc.* 40:1361.
- Li X, Xu Q, Han G, Zhu W, Chen Z, He X, Tian X (2009). Equilibrium and kinetic studies of copper (II) removal by three species of dead fungal biomasses. *J. Hazard. Mater.* 165:469-474.
- Maldonado MI, Malato S, Perez-Estrada LA, Gernjak W, Oller I, Domenech X, Ali S, Hussain T, Nawaz R (2006). Optimization of alkaline extraction of natural dye from Henna leaves and its dyeing on cotton by exhaust method. *J. Clean. Prod.* 17:61-66.
- Malik PK (2003). Use of activated carbons prepared from sawdust and rice-husk for adsorption of acid dyes a cause study of Acid yellow. 36. *Dyes. Pigm. J.* 56:239-249.
- McKay G, Blair HS, Gardener JR (1982). Adsorption of dyes on chitin. I. Equilibrium studies. *J. Appl. Polym. Sci.* 27:3043-3057.
- Mourão PAM, Laginhas C, Custódio F, Nabais JMV, Carrott PJM, Ribeiro Carrott, MML (2011). Influence of oxidation process on the adsorption capacity of activated carbons from lignocellulosic precursors. *Fuel. Process. Technol.* 92:241-246.
- Navalon A, Prielo A, Araujo L, Vilchez JL (2002). Determination of oxadiazon residues by headspace solid-phase micro-extraction and gas chromatography-mass spectrometry. *J. Chromatogr. A.* 946:239-245.
- Nickolov R, Mehandjiev D (2000). The simplified equation for micropore size distribution in adsorbents with different texture and chemical nature. In: *Proceeding of 9th International Symposium of Catalysis, Varna*, pp. 193-198.
- Omri A, Wali A, Benzina M (2012). Adsorption of bentazon on activated carbon prepared from Lawsonia inermis wood: Equilibrium, kinetic and thermodynamic studies. *Arabian. J. Chem.*
- Pant KK, Singh TS (2004). Equilibrium, kinetics, and thermodynamics, study for adsorption of As (III) ions on activated alumina. *Sep. Purif. Technol.* 36:139-147.
- Pappiernik S, Yates S, Koskinen W, Barber B (2007). Processes affecting the dissipation of the herbicide Isoxafutole and its diketonitrile metabolite in agricultural soils under field conditions. *J. Agric. Food. Chem.* 55:8630-8639.
- Pintar A (2005). Catalytic processes for the purification of drinking water and industrial effluents. *Catal. Today.* 77:451-465.
- Pourata R, Khataee AR, Aber S, Daneshvar N (2009). Removal of the herbicide bentazon from contaminated water in the presence of synthesized nanocrystalline TiO powders under irradiation of UV-C light. *Desalination.* 249:301-307.
- Rajashekara MHM, Monomania HK (2007). Aerobic degradation of technical hexachlorocyclohexane by a defined microbial consortium. *J. Hazard. Mater.* 149:18-25.
- Ren L, Zhang J, Li Y, Zhang C (2011). Preparation and evaluation of cattail fiber-based activated carbon for 2, 4-dichlorophenol and 2, 4, 6-trichlorophenol removal. *Chem. Eng. J.* 168:553-561.
- Saritha P, Aparna C, Himabindu V, Anjaneyulu Y (2007). Comparison of various advanced oxidation processes for the degradation of 4-chloro-2 nitrophenol. *J. Hazard. Mater.* 149:609-614.
- Simal S, Castell-Palou A, Rossellet C (2007). Water desorption thermodynamic properties of principal. *J. Food. Eng.* 80: 1293-1301.
- Singh S, Lokesh KV, Sambhi SS, Sharma SK (2008). Adsorption Behaviour of Ni (II) from Water onto Zeolite X: Kinetics and Equilibrium Studies. *Proceedings of the World Congress on Engineering and Computer Science 2008 WCECS 2008, October 22-24, San Francisco, USA, ISBN: 978-988-98671-0-2.*
- Tsami C (1991). Net isosteric heat of sorption in dried fruits. *J. Food. Eng.* 14:325-327.
- Wang SL, Tzou YM, Lu YH, Sheng G (2007). Removal of 3-chlorophenol from water using rice-straw-based carbon. *J. Hazard. Mater.* 147:313-318.
- Weber TW, Chakraborti RK (1974). Pore and solid diffusion models for fixed bed adsorbents. *J. Aiche.* 20:228-238.
- Zhang Wei-P, Yang Yong-Q, Li M-xuan, et al. (2010). Abdominal Ultrasonic Manifestations of 284 Occupational Organophosphorus Pesticide Contacts. *Practical Preventive medicine.* ISSN 1006-3110. 17:4pp.
- Zhu JL, Hjollund NH, Andersen AM, Olsen J (2006). Occupational exposure to pesticides and pregnancy outcomes in gardeners and farmers: a study within the Danish National Birth Cohort. *J. Occup. Environ. Med.* 4:347-352.